Journal of Alloys and Compounds 509 (2011) 72–75

Contents lists available at ScienceDirect

Journal of Alloys and Compounds

journal homepage: www.elsevier.com/locate/jallcom

Synthesis and luminescence studies of CdSrS nanostructures

Puja Chawla[a,*], S.P. Lochab[b], Nafa Singh[a]

[a] Department of Physics, Kurukshetra University, Kurukshetra 136 119, India
[b] Inter University Accelerator Centre, Aruna Asaf Ali Marg, New Delhi 110 067, India

ARTICLE INFO

Article history:
Received 24 April 2010
Received in revised form 20 August 2010
Accepted 24 August 2010
Available online 29 September 2010

Keywords:
Nanostructures
Transmission electron microscopy
X-ray diffraction

ABSTRACT

Cadmium strontium sulfide nanostructures were synthesized by solid state diffusion method in the presence of sodium thiosulfate. XRD confirmed the presence of CdS and SrS structures in the synthesized samples. TEM micrographs revealed the formation of nearly spherical nanoparticles with grain size in the range 30–40 nm. The PL emission was centred around 532 nm with a shoulder at 468 nm. The PL emission of CdSrS shows a blue shift in comparison to that of CdS. Substantially enhanced photoluminescence emission was observed with the addition of Bi^{3+} as a dopant. The effects of different excitation wavelengths on the PL spectra have also been investigated. It is suggested that the emission processes are linked to divalent Cd ions with broadening resulting due to these ions in being differing ion environments.

1. Introduction

In recent years, hybrid materials have received growing research interests, since they usually provide a new functional hybrid with synergistic or complementary activity between each constituent, which are not available from their single components, and can provide novel or enhanced properties for various applications [1,2]. Especially, sulfide hybrid materials have attracted considerable attention because of their unique luminescence, magnetic, electrical and photocatalytic properties [3–6]. Semiconductor photocatalysis has been intensively studied recently especially the binary metal chalcogenides of group II^B such as CdS [7–9], ZnS [10] and PbS [11], because of their novel properties as a consequence of the large number of surface atoms and the three dimensional confinement of electrons [12–14]. The dual semiconductor systems such as ZnS–CdS, CdS–TiO_2, CdS–ZnO, ZnO–ZnSe and CdS–HgS are known to exhibit higher photocatalytic activity as compared to their constituent sulfides or oxides [15,16]. Recently the ternary compounds of CdS and ZnS viz $Cd_xZn_{1-x}S$ are investigated as promising materials for high-density optical recording and short wavelength laser diode applications [17]. However, with different preparative routes such alloys have shown narrow or broad photoluminescent emission. Particular interest has been invoked in alloyed systems such as $Ca_{1-x}Cd_xS$ where Lehmann [18], Ray et al. [19] and Barrett et al. [20] have observed immensely enhanced luminescence emission both in terms of intensity and spectral distribution. However, within the limits of our knowledge, only few investigations have focused on this area.

More recently, we have reported the luminescence of undoped and Bi doped CdS [21] and SrS:Bi [22,23] nanostructures. The SrS compounds crystallize only in the rock salt structure which is incompatible with the zincblende or wurtzite structure in which II^B–VI^B compounds crystallize [24]. The resulting II^B–II^A–VI^B compound is generally thought to form an immiscible system, hence the investigation for these compounds is very limited and therefore many fundamental aspects in optoelectronic properties of these compounds are not yet unveiled. Thus, combining the advantages of SrS and CdS to fabricate a promising novel system may provide a new functional hybrid between each constituent. Systematic luminescence studies of CdSrS (group II^B–II^A–VI^B) nanostructures have been reported in this paper. The solid state diffusion method has been used for the synthesis of CdSrS nanostructures in the presence of sodium thiosulfate. The advantage of this method is that synthesis can be done on a large scale with a little chance of undesired impurities. The effect of excitation wavelengths and Bi doping on PL intensity has also been investigated. To the best of our knowledge, the effect of Bi doping on PL intensity has been investigated for the first time in CdSrS nanophosphors. These products have been characterized by X-ray diffraction (XRD), transmission electron microscopy (TEM), and photoluminescence (PL) spectroscopy.

2. Synthesis

We adopted the solid state diffusion method [25] to synthesize CdSrS and CdSrS:Bi nanostructures. Depending upon the initial precursors used for the synthesis, CdSrS may be prepared by the following two techniques:

* Corresponding author.
E-mail address: ranu.puja@gmail.com (P. Chawla).

0925-8388/$ – see front matter © 2010 Elsevier B.V. All rights reserved.
doi:10.1016/j.jallcom.2010.08.084

Method-1: This method involves the reduction of sulfate using carbon powder into its sulfide form and then incorporation of an activator into the lattice in the presence of a suitable flux at a high temperature. We procured cadmium sulfate, strontium sulfate, sodium thiosulfate, bismuth nitrate, and carbon powder of analytical grade. Carbon powder was soaked in excess of deionized distilled water for about half an hour, then dried in an oven and finally collected in a clean bottle. Appropriate proportions of the ingredients cadmium sulfate, strontium sulfate and carbon powder were taken together in a clean agate pestle and mortar. We used clean graphite crucibles and a thin layer of carbon powder was spread over the charge to keep a reducing atmosphere. The firing was carried out in a muffle furnace provided with an automatic temperature control. The final firing temperature was 1000 °C and the firing time was 2 h. After firing, the charge was transferred to a mortar and was rapidly pulverized while red hot. The phosphor powder was then collected in a clean and dry sample bottle. Samples of CdSrS:Bi were prepared in the same way as described above with the desired concentration of the activator. The required amount of bismuth nitrate (0.05 mol%) was added to the charge and then mixed again for some time before firing the whole charge.

Method-2: The starting materials, CdS [21], SrS [23], $Bi(NO_3)_3{\cdot}5H_2O$ and S (A.R. grade), were weighed and mixed to obtain the prescribed composition. Mixing was accomplished in an agate pestle and mortar and the charge was put in a graphite crucible. Sulfur was added in the mixture to provide a sulfurising atmosphere. The firing was carried out in a muffle furnace provided with an automatic temperature control. The final firing temperature was 1000 °C and the firing time was 2 h. After firing, the charge was transferred to a mortar and was rapidly pulverized while red hot. The phosphor powder was then collected in a clean and dry sample bottle. Samples of CdSrS:Bi were prepared in the same way as described above with the required amount of activator. Bismuth nitrate (0.05 mol%) was added to the charge and then mixed again for some time before firing the whole charge.

The morphology and sizes of the product were determined by TEM carried out using a H-7500 model (Hitachi Ltd., Tokyo, Japan) operated at 100 kV. Diluted nanoparticles suspended in absolute ethanol were introduced on a carbon coated copper grid, and were allowed to dry in air for conducting the TEM studies. The phase purity of the samples was confirmed by XRD studies through the use of a Bruker Advance D8 X-ray diffractometer using Cu Kα radiation. PL was recorded with a Fluoro Max-3 (Jobin–Yvon, Edison NJ, USA) equipped with a photomultiplier tube and a Xenon lamp of 150 W.

3. Results and discussion

Fig. 1 shows the XRD patterns of CdSrS and CdSrS:Bi nanostructures, which indicates the presence of both CdS and SrS phases without any noticeable traces of impurity. The diffraction lines of the cubic phase of SrS (JCPDS file no. 08-0489), cubic phase of CdS (JCPDS file no. 10-454) and hexagonal phase of CdS (JCPDS file no. 80-0006) have also been depicted for comparison. From the X-ray powder diffraction measurements the cubic phase was observed as the dominant phase in all these samples. However, for the samples prepared by method-1 there were traces of the hexagonal lines of CdS present. A comparison of intensity relative to the rock salt lines suggested evidence of a few mole percent of CdS, whereas, for the samples prepared by method-2, the cubic phase of CdS has been observed. Thus, the CdS phase in CdSrS samples prepared by two methods varies. Since, the ionic radius of Sr^{2+} is larger than that of the Cd^{2+} ion, the decomposition into two phases occurred. Here complete miscibility was not expected because the atomic radii and electronegativity of Sr and Cd are not within the limits set by Hume–Rothery rules [26]. But, the photoluminescence

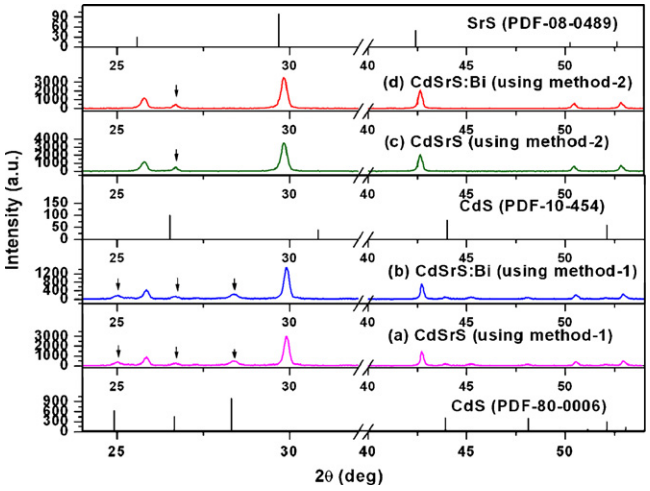

Fig. 1. X-ray diffraction patterns of CdSrS (a), CdSrS:Bi (b) using method-1; and CdSrS (c), CdSrS:Bi (d) using method-2.

results clearly revealed that Sr-doping can efficiently improve the emission characteristics of CdS.

Fig. 2(a) and (b) shows the PL emission for CdSrS phosphors prepared by method-1 and method-2, respectively. From these figures, we can clearly observe that CdSrS synthesized by method-2

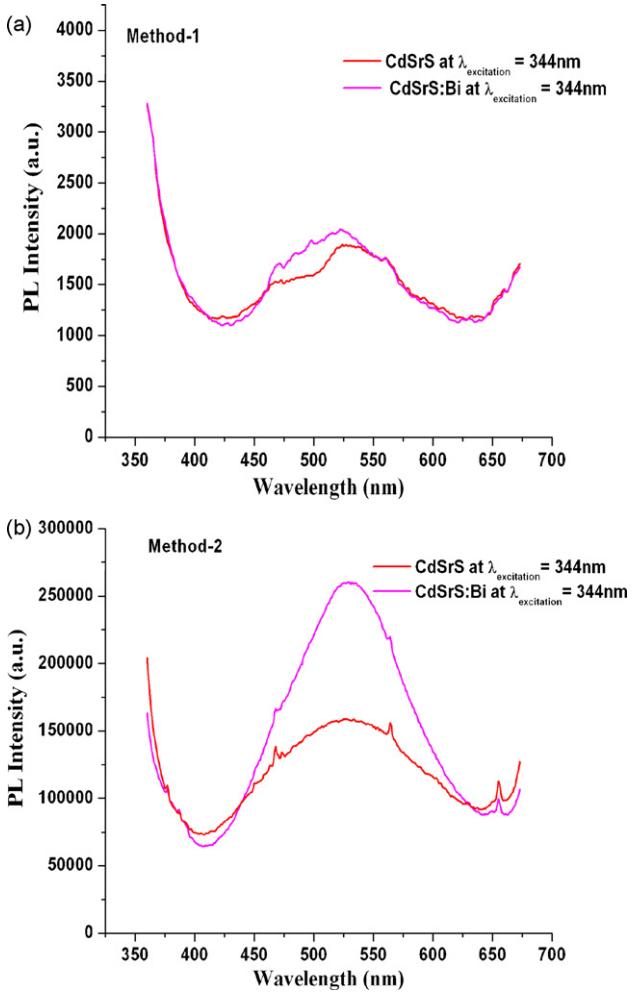

Fig. 2. PL emission spectra of CdSrS and CdSrS:Bi nanophosphors synthesized by (a) method-1 and (b) method-2.

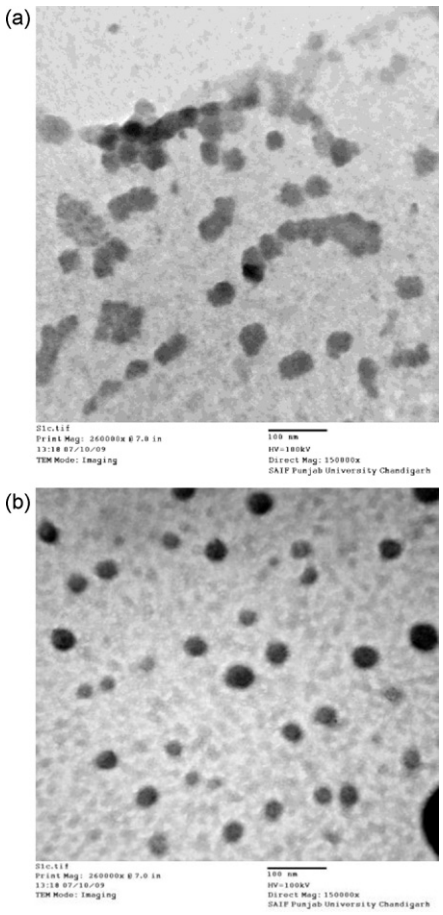

Fig. 3. TEM micrographs of (a) CdSrS and (b) CdSrS:Bi.

gives an enhanced PL emission as compared to method-1. Thus, CdSrS phosphor synthesized using method-2 was chosen for further investigation. Further, the addition of Bi as activator shows an abrupt increase in the emission intensity. The TEM micrographs of CdSrS and CdSrS:Bi nanoparticles synthesized by method-2 are shown in Fig. 3, which indicates nearly spherical morphology of the samples. The average crystallite sizes are 40 nm and 35 nm respectively with distribution in the range 30–40 nm.

The PL spectra for CdSrS excited at 344 nm, shows emission centred around 532 nm with small humps at 468 nm and 560 nm. While pure SrS is almost nonluminescent; addition of CdS causes the appearance of an emission which may easily be the broadest ever measured in any phosphor, it extends from almost (λ = 390 nm) in the ultraviolet to about (λ = 700 nm) in the infrared as shown in Fig. 2. A superposition of several bands in the spectrum may be present but it is not clearly resolved. This emission may be explained in terms of local lattice deformations [19]. Pure CdS normally crystallizes as wurtzite in which every Cd-ion is tetrahedrically surrounded by four S-ions. SrS has, of course, rock salt structure in which each Sr-ion is octahedrically surrounded by six S-ions. However, clusters of several Cd-cations are likely to be present in intermediate CdS–SrS, even if the former is completely randomly distributed in the lattice, and the tendency toward tetrahedral configuration may be strong enough in such clusters to cause local lattice disturbances which may be the centres of luminescence. Photoluminescence results showed that Sr-doping can efficiently improve the emission characteristics of CdS.

Fig. 4 shows the PL spectra for CdSrS:Bi as a function of exciting wavelengths in the range 250–365 nm. It can be seen that for excitation at 250 nm, the emission peaks at 390 nm and 468 nm have

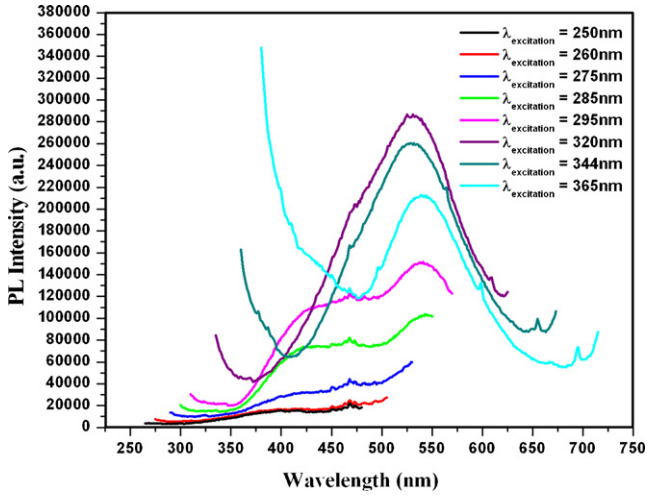

Fig. 4. Photoluminescence spectra of CdSrS:Bi nanoparticles at different excitations between 250 nm and 365 nm.

been observed and these peaks show a red shift as excitation wavelength increases. There was a large shift in emission wavelength from 468 nm to 540 nm as the excitation wavelength changes from 275 nm to 285 nm. As the excitation wavelength was increased further, the peak was at 532 nm with a shoulder at 468 nm. At 365 nm, the PL emission between 390 nm and 468 nm has fallen to zero, whereas the emission at 538 nm identified with the band edge of bulk CdS is clearly visible. Thus the emission region of CdSrS varies from 390 nm to 538 nm (i.e. from ultraviolet to green (For interpretation of the references to wavelength in this text, the reader is referred to the web version of the article.)) with the excitation wavelength as shown in Fig. 4 and tabulated in Table 1. Thus, the blue/green ratio decreases as the excitation wavelength increases. This is broadly in line with previous observations in CaS lattice [20]. This is indicative of a progressive random distribution of cadmium and strontium sub-lattices with a shift in band location in k-space arising from the introduction of an indirect band gap, SrS into the CdS lattice. Broadening in the emission peaks reflect a greater spread of intra-band states associated with the excitation and emission processes of clustering of SrS within the CdS lattice.

Fig. 5(a) compares the PL spectra of CdSrS and CdSrS:Bi excited at 420 nm. It can be seen that for excitation at 420 nm, CdSrS does not give any emission, whereas the emission centred around 468–532 nm is still clearly visible in case of CdSrS:Bi identifying the presence of Bi. Fig. 5(b) shows the excitation spectra of both CdSrS and CdSrS:Bi for the 535 nm emission peak as supporting information for the emission spectra of Fig. 5(a). We have previously reported the emission of pure CdS [21] at 550 nm with a shoulder at 620 nm, CdS:Bi at 413 nm with CdS emission ranging from 500 nm to 700 nm and SrS:Bi [23] emission at 481 nm. Earlier, Lehmann [18] have focused on the effect of Cd on the optical absorption edge of CaS lattice. The shift in emission peaks observed in the present

Table 1
PL emission wavelengths at different excitation wavelengths for CdSrS:Bi nanophosphors in the interval 250 nm and 365 nm.

$\lambda_{Excitation}$ (nm)	$\lambda_{Emission}$ (nm)
250	390, 468
260	400, 468
275	421, 468
285	421, 540
295	434, 538
320	468, 530
344	468(very small), 532
365	538

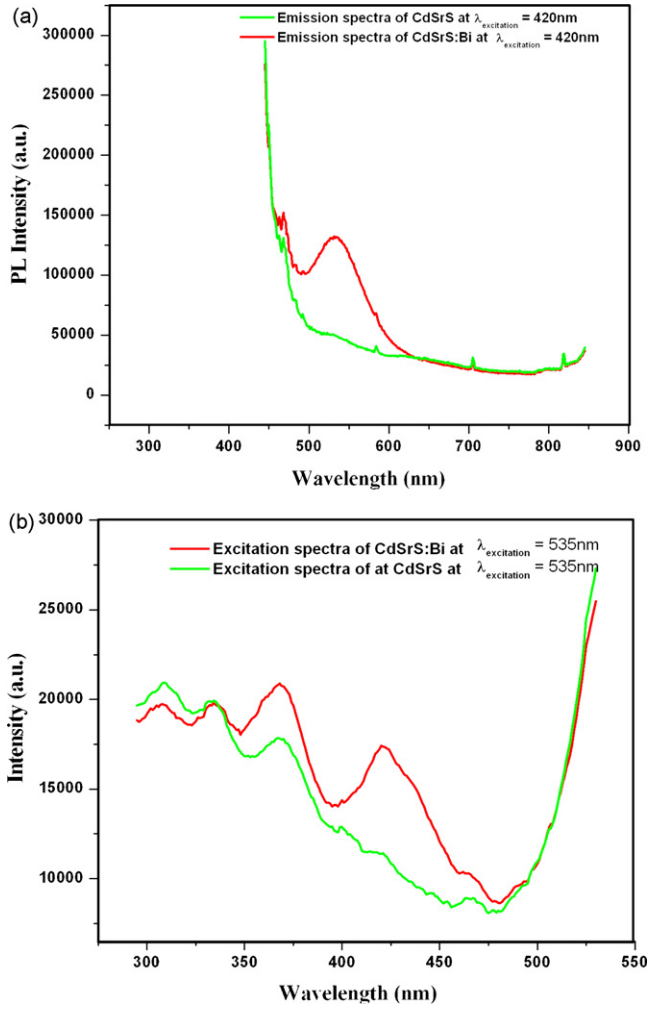

Fig. 5. (a) PL emission spectra of CdSrS and CdSrS:Bi at an excitation wavelength of 420 nm and (b) excitation spectra at an emission wavelength of 535 nm.

case is totally in tune with Lehmann's observations of an abrupt “band edge” shift in CaS pointing to the effect of Cd on the conduction band edge and its consequent relation to associated emitting centres. The results of the present studies also proved that SrS and CdS in the composite form were not simple physical mixture [27], but they had a synergistic effect on various properties.

4. Conclusions

CdSrS nanostructures have been synthesized by the solid state diffusion method in the presence of sodium thiosulfate. TEM pictures reveal nearly spherical morphology with size distribution in the range 30–40 nm. PL emission for these nanostructures is at 532 nm with slight shoulder at 468 nm at an excitation of 344 nm. The PL emission intensity shows an abrupt increase with the addition of Bi to CdSrS lattice. The blue/green ratio decreases as the excitation wavelength increases. This is linked to the random distribution of cadmium and strontium sub-lattices with a shift in band location in k-space arising from the introduction of an indirect band gap, SrS into the CdS lattice.

References

[1] J. Jiang, L.H. Ai, J. Alloys Compd. 502 (2010) 488–490.
[2] L.P. Marushko, Y.E. Romanyuk, L.V. Piskach, O.V. Parasyuk, I.D. Olekseyuk, S.V. Volkov, V.I. Pekhnyo, J. Alloys Compd. 505 (2010) 101–107.
[3] J.K. Dongre, M. Ramrakhiani, J. Alloys Compd. 487 (2009) 653–658.
[4] S. Zu, Z. Wang, B. Liu, X. Fan, G. Qian, J. Alloys Compd. 476 (2009) 689–692.
[5] Y. Li, R. Yi, X. Liu, J. Alloys Compd. 486 (2009) L1–L4.
[6] S. Arora, S.S. Manoharan, Opt. Mater. 31 (2008) 176–180.
[7] R. Banerjee, R. Jayakrishnan, P. Ayub, J. Phys.: Condens. Matter 12 (2000) 10647–10654.
[8] H.M. Wang, P.F. Fang, Z. Chen, et al., J. Alloys Compd. 461 (2008) 418–422.
[9] P. Chawla, G. Sharma, S.P. Lochab, N. Singh, Radiat. Eff. Defects Solid 164 (2009) 755–762.
[10] Z.J. Li, W.Z. Shen, L.M. Fang, et al., J. Alloys Compd. 463 (2008) 129–133.
[11] Z.I. Xiu, S.W. Liu, J.X. Yu, et al., J. Alloys Compd. 457 (2008) 9–11.
[12] A. Henglein, Chem. Rev. 89 (1989) 1861–1873.
[13] Y. Wang, N. Herron, J. Phys. Chem. 95 (1991) 525–532.
[14] A. Eychmuller, J. Phys. Chem. B 104 (2000) 6514–6528.
[15] P.V. Kamat, J. Phys. Chem. C 111 (2007) 2834–2860.
[16] N.A. Noor, N. Ikram, S. Alia, S. Nazir, S.M. Alay-e-Abbas, A. Shaukat, J. Alloys Compd. (2010), doi:10.1016/j.jallcom.2010.07.197.
[17] S. Guha, B.J. Wu, H. Cheng, J.M. Depuydt, Appl. Phys Lett. 63 (1993) 2129–2131.
[18] W. Lehmann, J. Lumin. 5 (1972) 87–107.
[19] B. Ray, J.W. Brightwell, D. Allsop, A.G.J. Green, J. Cryst. Growth 86 (1988) 644–649.
[20] E. Barrett, G.R. Fern, B. Ray, R. Withnall, J. Silver, J. Opt. A: Pure Appl. Opt. 7 (2005) S265–S269.
[21] P. Chawla, S.P. Lochab, N. Singh, J. Alloys Compd. 492 (2010) 662–666.
[22] P. Chawla, S.P. Lochab, N. Singh, J. Alloys Compd. 494 (2010) L20–L24.
[23] P. Chawla, S.P. Lochab, N. Singh, Mater. Res. Bull. 45 (2010) 783–786.
[24] K. Zhang, D. Jing, Q. Chen, L. Guo, Int. J. Hydrogen Energy 35 (2010) 2048–2057.
[25] V. Singh, T.K. Gundu Rao, J.J. Zhu, M. Tiwari, Mater. Sci. Eng. B 131 (2006) 195–199.
[26] A.J. Dekker, Solid State Physics, Prentice-Hall Inc., Englewood Cliffs, New Jersey, 1957.
[27] H. Liu, K. Zhang, D. Jing, G. Liu, L. Guo, Int. J. Hydrogen Energy (2010), doi:10.1016/j.ijhydene.2010.01.028.